Research Article

Hui Li, Rongzheng Xu*, Yanxi Hou, Shenglin Cui, and Zhicheng Wei

Feasibility and interface migration characteristics of friction stir lap welding of LA141 Mg-Li alloy

https://doi.org/10.1515/rams-2019-0015
Received Nov 09, 2018; accepted Feb 18, 2019

Abstract: 2 mm-thick LA141 plates were successfully friction stir lap welded (FSLW). The similar FSLW LA141 Mg-Li alloy joint appeared a downward hook on the advanced side and an upward cold lap on the retreating side. The load of lap-shear tensile testing reached 2.8 kN, and the joints failed in the interface defects. The interface migration of LA141/LA141 lap joint during FSLW process was driven by forces at interface, such as a frictional force paralleled to the thread, a downward pressure perpendicular to the surface of the thread, the resistance from unsoftened metal and its own gravity. Moreover, the FSLW of AZ31/LA141 and LA141/AZ31 furtherly verified that forces at the interface were critical factors in determining the interface migration during FSLW process.

Keywords: Mg-Li alloy, FSLW, property, interface migration

1 Introduction

Mg-Li alloys are the lightest structural metal with remarkable properties such as superior specific strength, high elastic modulus and good recyclability, which meet the increasing global mandates of fuel saving and greenhouse gas emissions [1]. Their densities are only 1.35~1.65g/cm^3, 1/4 to 1/3 lighter than that of the ordinary Mg alloys [2]. In addition, when considering their good bending stiffness and high specific strength, Mg-Li alloys make them attractive and promising for aerospace industry [3]. However, it should be pointed out that Li is chemically active in nature and easily burned during fusion welding, and the consequent Mg-Li joint is more prone to form weld defects compared to other Mg alloys at an elevated temperature [4]. A suitable welding technology is therefore essential to promote the industrialization of Mg-Li alloys.

As a solid-state joining method, friction stir welding (FSW) in contrast to fusion welding has been proven to be a potential welding technique for joining Mg-Li alloys [5, 6]. During the FSW process of Mg-Li alloys, the problems such as volatilization of Li element and reaction with other gases associated with fusion welding can be avoided because of the formation of a self-closing system between the welding tool and the welded material, which makes it possible to realize a robust butt joint [7–10].

Besides the butt joint, the lap joint is another important joining configuration for automotive and aerospace industries. At present, for FSLW of ordinary Mg alloys, the hook on the advancing side (AS) and cold lap on the retreating side (RS) formed by the interface migration, obviously limited the mechanical properties of the joint [11]. Research indicated that the different physical properties, such as melting point and density between different Mg alloys, are highly influential on the material flow behavior during FSLW, affecting the interface morphology [12–14]. However, there are currently little researches on FSLW of Mg-Li alloys and their interface migration during FSLW, restricting their industrial application to some extent.

In this study, 2.0 mm-thick LA141 Mg-Li alloy plates were selected as substrate material to investigate the feasibility of FSLW to join Mg-Li alloys. On this basis, the interface migration characteristics of the FSLW LA141/LA141 joint were evaluated, and were furtherly verified by the FSLW AZ31/LA141 and LA141/AZ31 joints.

2 Experimental

In this study, LA141 Mg-Li alloy plates and AZ31B Mg alloy plates, 300 mm×150 mm×2.0 mm in dimension, were employed as base materials (BMs). Their chemical compositions and mechanical properties were listed in Tables 1 and 2, respectively.

***Corresponding Author: Rongzheng Xu:** College of Material Science and Engineering, Shenyang Aerospace University, 37 Daoyi South Street, Shenyang, 110136, China; Email: rzxu@imr.ac.cn, Tel.: 86–24–89724198, Fax: 86–24–89724198
Hui Li, Yanxi Hou, Shenglin Cui, Zhicheng Wei: College of Material Science and Engineering, Shenyang Aerospace University, 37 Daoyi South Street, Shenyang, 110136, China

Table 1: Chemical compositions of LA141 Mg-Li alloy and AZ31 Mg alloy (mass, %).

Material	Mg	Li	Al	Zn	Mn	Ca	Cu	Ni	Fe
AZ31	Bal.	-	3.11	0.68	0.47	<0.04	<0.05	<0.005	-
LA141	Bal.	14.9	1.31	-	0.13	0.001	0.001	-	0.005

Table 2: Mechanical properties of LA141 Mg-Li alloy and AZ31 Mg alloy.

Material	Tensile strength, MPa	Elongation, %	Hardness, Hv	Melting point, °C	Density, g/m^3	Thermal conductivity, w/m·k
LA141	227	30	40	580	1.35	80.0
AZ31	256	10	49	650	1.77	155.5

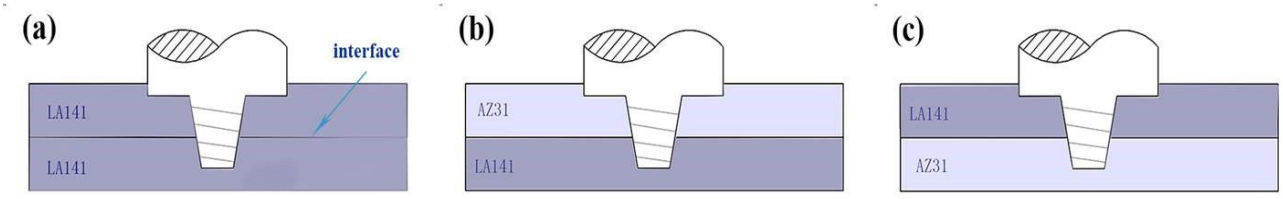

Figure 1: The lap configurations: FSLW of (a) LA141/LA141 (b) AZ31/LA141 and (c) LA141/AZ31.

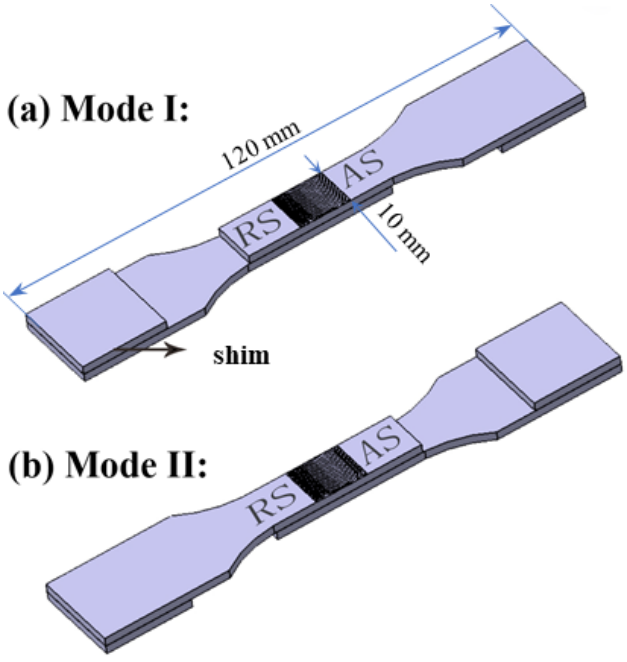

Figure 2: Two different loading modes: (a) Mode I and (b) Mode II.

Prior to welding, the overlapped regions were polished using emery papers to break down existing surface oxides and wiped with alcohol. In this experimental setup, two plates were overlapped with a lap width of 40 mm. All the welding experiments were carried out using an FSW machine (FSW-5LM-020), and three different lap configurations were shown in Figure 1. Consequently, there were three types of lap configurations: LA141/LA141, AZ31/LA141 and LA141/AZ31. To ensure the repeatability of results and stabilize the FSLW process, workpieces were tightly fixed in the workbench with clamps, while the shoulder plunged into the upper sheet by a prescribed plunge depth of 0.2 mm. All the FSLW operations were conducted at a rotational speed of 800 rpm and a travel speed of 400 mm/min.

After welding, the specimens were cut by an electrical discharge cutting machine, using for macrostructural observations and mechanical testing. The specimens were etched with acetic acid solution (7 mL acetic acid + 100 mL H_2O) and then the macrographs showing the weld profiles and the micrographs were acquired with an optical microscopy (OM). Due to the asymmetric characteristic of the FSLW joint, two welding orientations were introduced, resulting in two different loading modes as schematically illustrated in Figure 2. In Mode I, the probe is always located near AS of the top plate edge, while in Mode II, the probe is always located near RS of the top plate edge. To balance the offset axes of the lap specimens and minimize the bending effect, two shims with the corresponding thickness of 2 mm were used during the lap-shear tensile testing. The average testing result of the LA141/LA141 lap joint was calculated and its typical fracture surface was examined by OM, while the fracture mode of different loading modes was investigated.

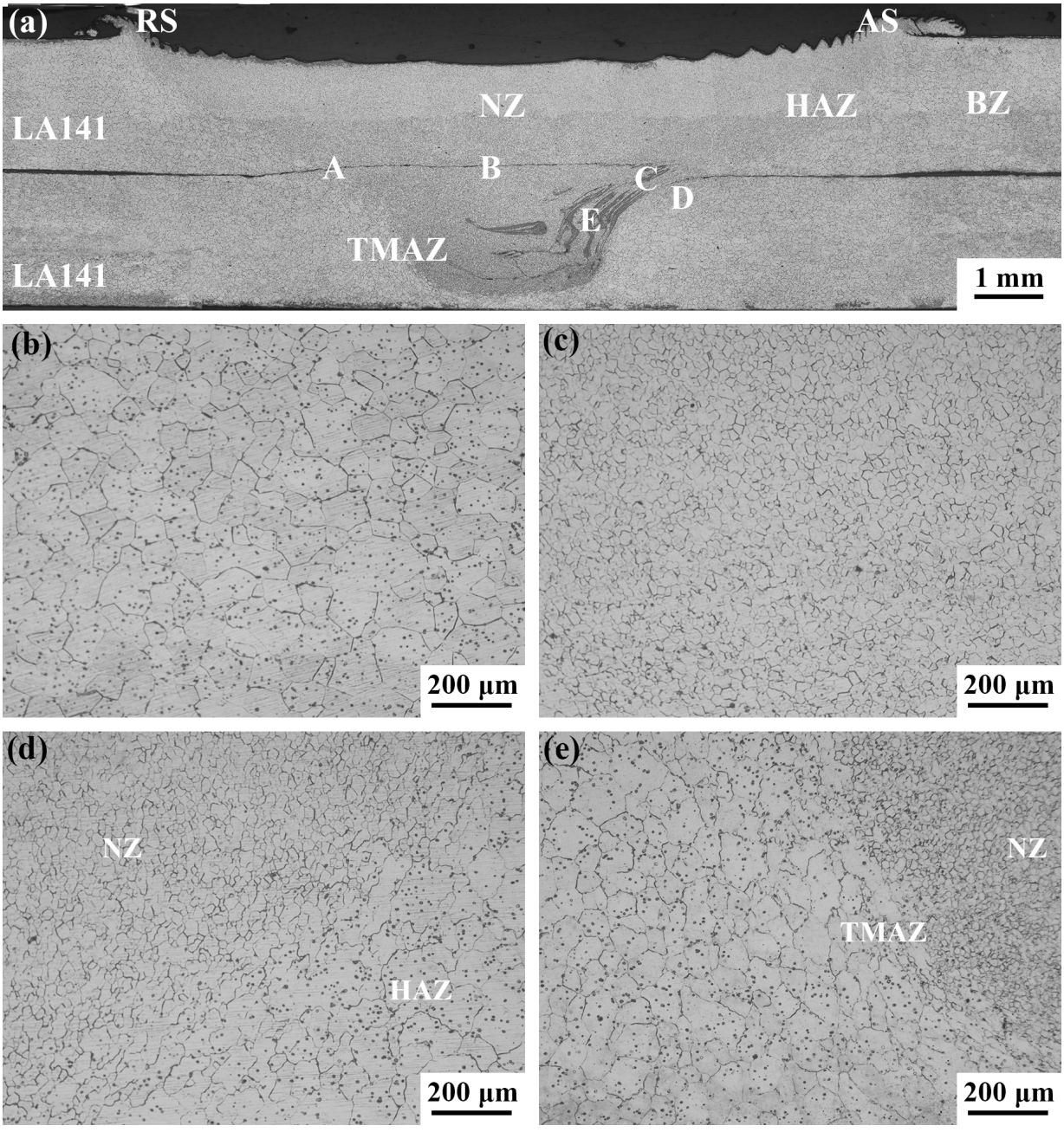

Figure 3: (a) Typical cross-section photograph of the LA141/LA141 lap joint and the microstructures of (b) BZ, (c) NZ, (d) HAZ and (e) TMAZ.

3 Results and discussion

3.1 Microstructure and the interface morphology

3.1.1 LA141/LA141 lap joint

Figure 3(a) exhibits the typical cross-sectional photograph of the LA141/LA141 lap joint, and no voids, cracks or other common weld defects were detected. The joint could be divided into four typical regions: the BM, the heat affected zone (HAZ), the thermo-mechanically affected zone (TMAZ) and the nugget zone (NZ). BM was mainly composed of homogeneous equiaxed grain, whose average size was about 30 μm as shown in Figure 3(b). In the NZ, high peak temperature and big strain rate occurred, which easily resulted in dynamic recrystallization and then obtained refined and equiaxed grains at about 10 μm (Figure 3(c)). In the meantime, the grain size gradually became smaller from the top to the bottom along thickness because

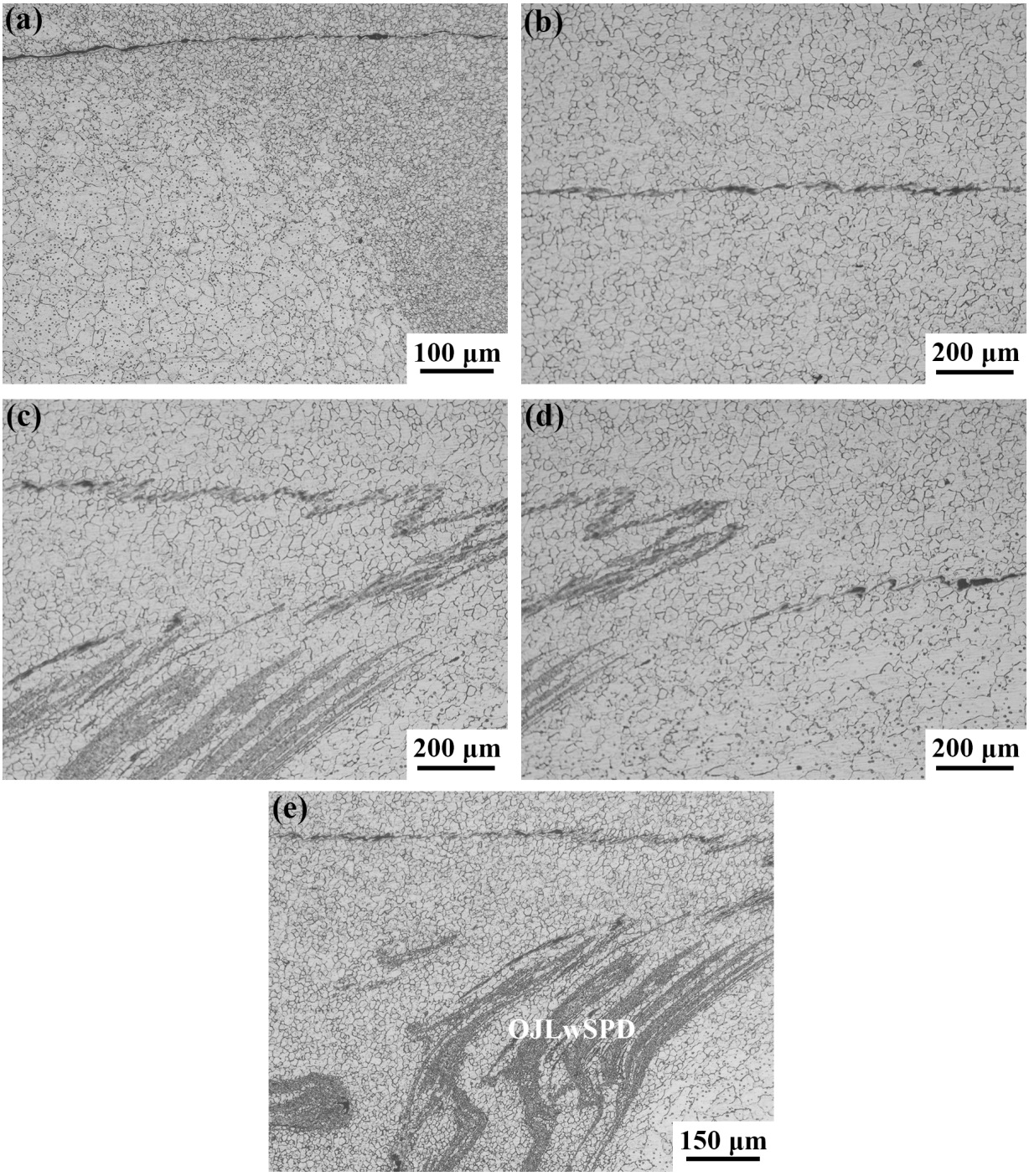

Figure 4: Magnified morphologies of (a) region A, (b) region B, (c) region C, (d) region D and (e) region E of joint in Figure 3a.

of significant temperature gradient (Figure 3(d) and 3(e)). Among the above observations, the closer that location is to the shoulder, the greater the heat input. In addition, in the HAZ without mechanical stirring but with high thermal cycle during FSLW, grains were coarsen reaching about 50 μm (Figure 3(d)), and grains in the TMAZ were elongated as shown in Figure 3(e).

As shown in Figure 4, defects such as hook (formed on the AS), cold lap (formed on the RS) and kissing bond were observed in the joint. The cold lap on the RS extended horizontally through the weld center to the boundary on the AS and showed a little upward bending, forming an intermittent connection layer at the interface (Figure 4(a), 4(b) and 4(c)), while the hook extended downwards and

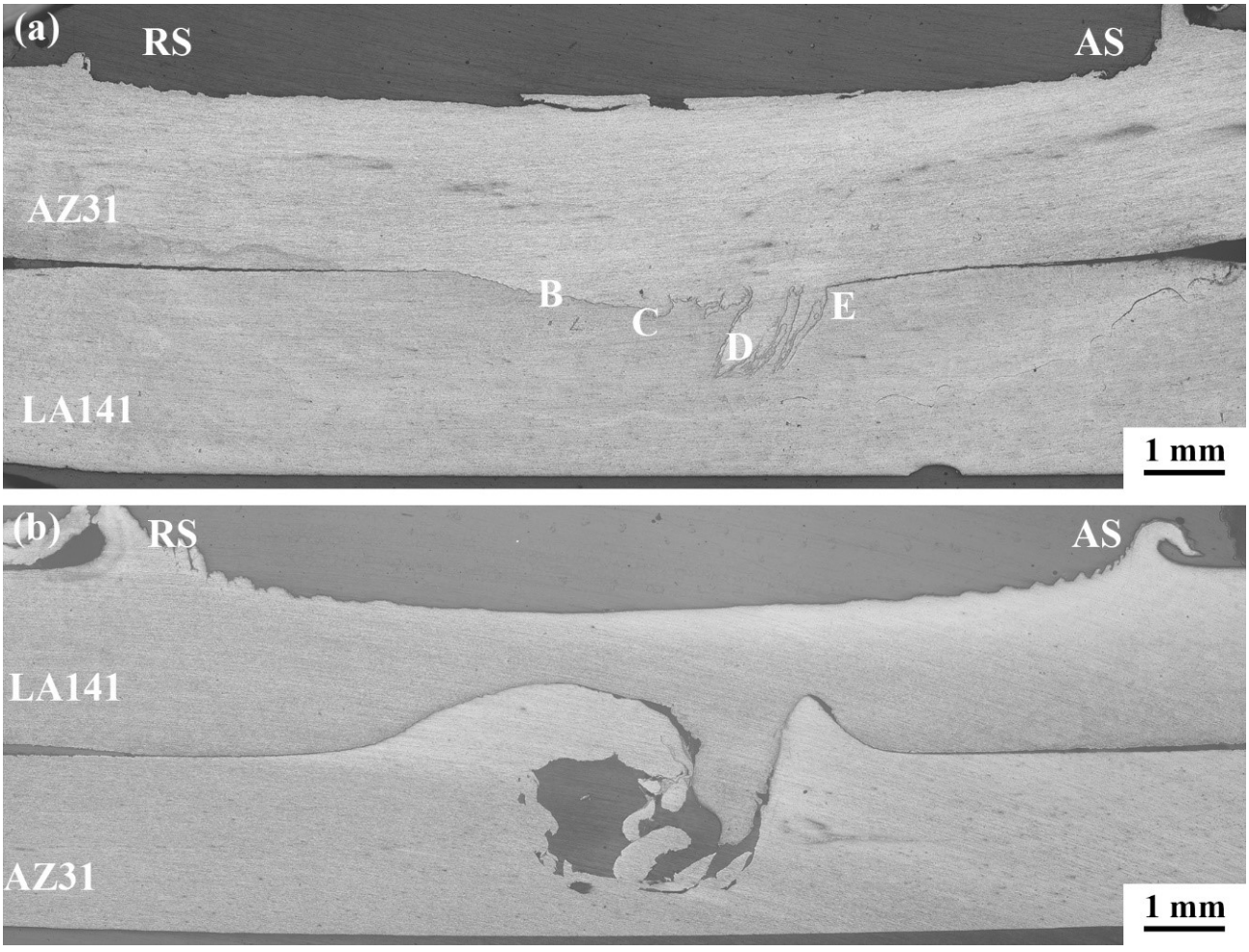

Figure 5: Typical cross-section photographs of FSLW (a) AZ31/LA141 and (b) LA141/AZ31 lap joints.

stopped at the NZ/TMAZ (Figure 4(d)). Additionally, a new defect, called kissing bond, resulted from the deformation of original faying interface. It was always characterized by broken oxide films at the end region of the cold lap (Figure 4(e)), which was remained in the stir zone and termed as "Original Joint Line with Severe Plastic Deformation (OJLwSPD)" [15, 16].

3.1.2 AZ31/LA141 and LA141/AZ31 lap joints

The AZ31/LA141 and LA141/AZ31 lap joints were introduced to understand the effect of physical properties of the BMs on interface migration characteristics of the joint. Therefore, only their interface morphologies were investigated in this study.

Figure 5(a) and (b) show the typical cross-sectional photographs of the AZ31/LA141 and LA141/AZ31 lap joints, respectively. It could be observed that the AZ31/LA141 lap joint was sound (Figure 5(a)), but the LA141/AZ31 lap joint, using the same welding parameters, appeared a hole defect (Figure 5(b)). In addition, there existed big differences on the interface morphology between two lap configurations. The cold lap on the RS of the AZ31/LA141 lap joint extended downwards slightly into the stir zone and further went towards the AS (Figure 6(a) and 6(b)). Near the AS, the oxides at the faying surface were transferred and presented a river feature as indicated in Figure 6(c). And the hook on the AS directed downwards at a bigger inclination angle towards the original faying surface and then arrested at the stir extremity (Figure 6(d)). In contrast, the cold lap in the LA141/AZ31 lap joint curved upwards as an arch to the core of the stir zone and stopped at the center of the weld hole (Figure 5(b)), while the hook presented an upward curve and then vertically descended at the extremity of the stir zone.

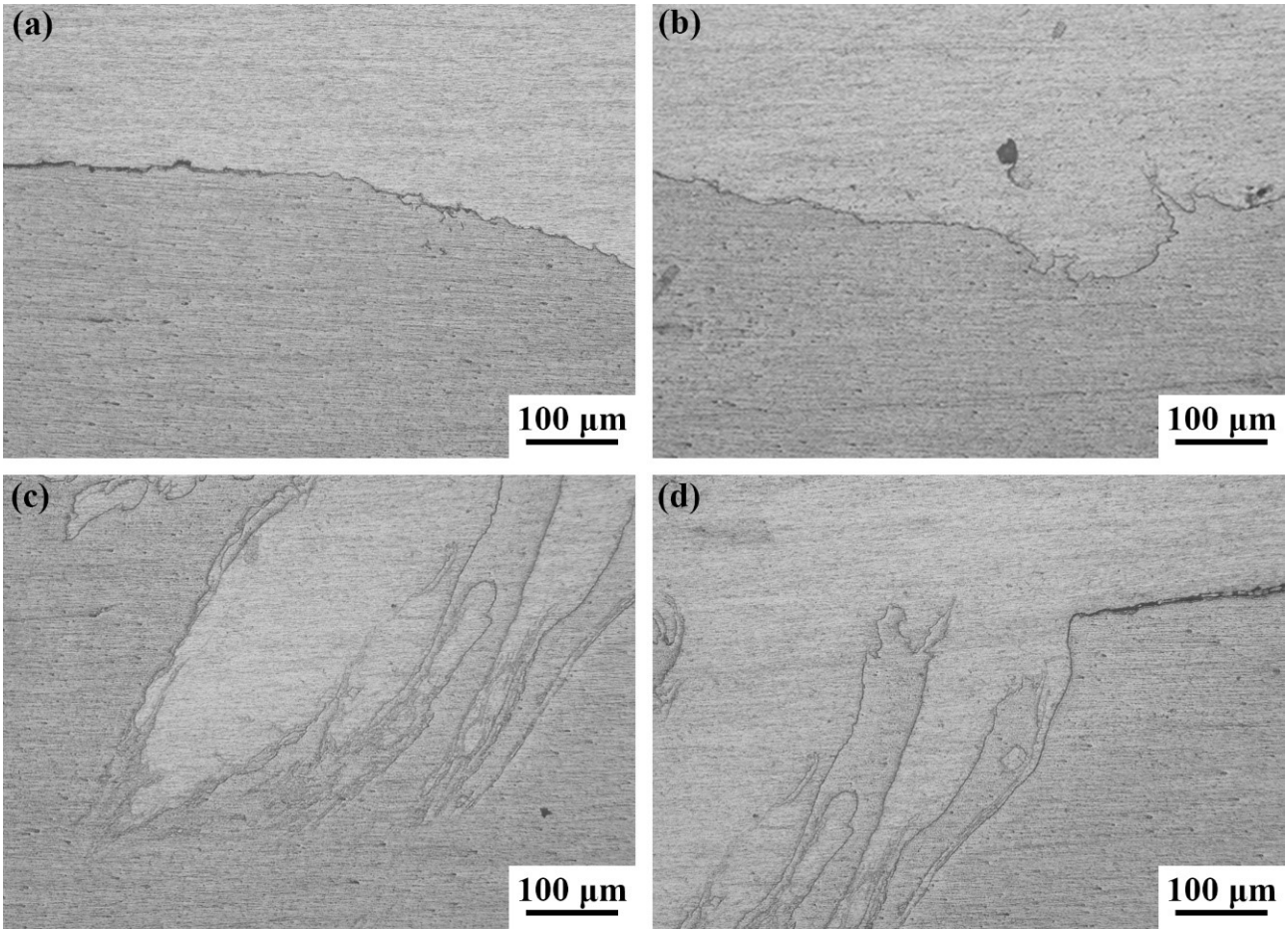

Figure 6: Magnified morphologies of (a) region B, (b) region C, (c) region D, and (d) region E in Figure 5(a).

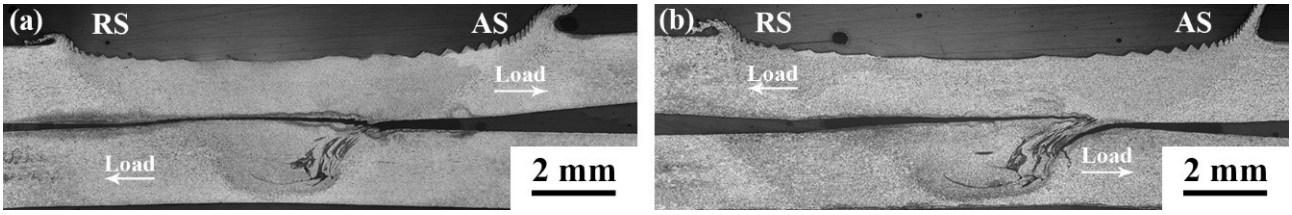

Figure 7: Fracture locations of the LA141/LA141 lap joints with two different loading modes: (a) Mode I and (b) Mode II.

3.2 Mechanical Properties of the LA141/LA141 lap joint

The fracture locations of the LA141/LA141 lap joint associated with two different loading modes are shown in Figure 7. In Mode I, the testing load was 2.3 kN and the joint failed in the lower plate along the hook, while in Mode II, the value reached 2.8 kN and the fracture was along the cold lap. Based on the fracture behaviors of the joint, the hook and cold lap played critical factors in affecting the mechanical properties of the joint. The hook extending into the NZ/TMAZ interface, causing sharp discontinuities at the interface and acute notches where the stress became highly concentrated, meanwhile leading to the reduction of the effective sheet thickness (Figure 7(b)). The cold lap was located in the TMAZ but extended into the stir zone, becoming the best path for crack propagation (Figure 7(a)).

The results of lap-shear tensile testing showed that the fracture direction and testing load of the LA141/LA141 lap joint were correlated to the interface morphology. However, the interface migration was usually related to the heat input and material flow behavior during FSLW, and it will be analyzed in the following section.

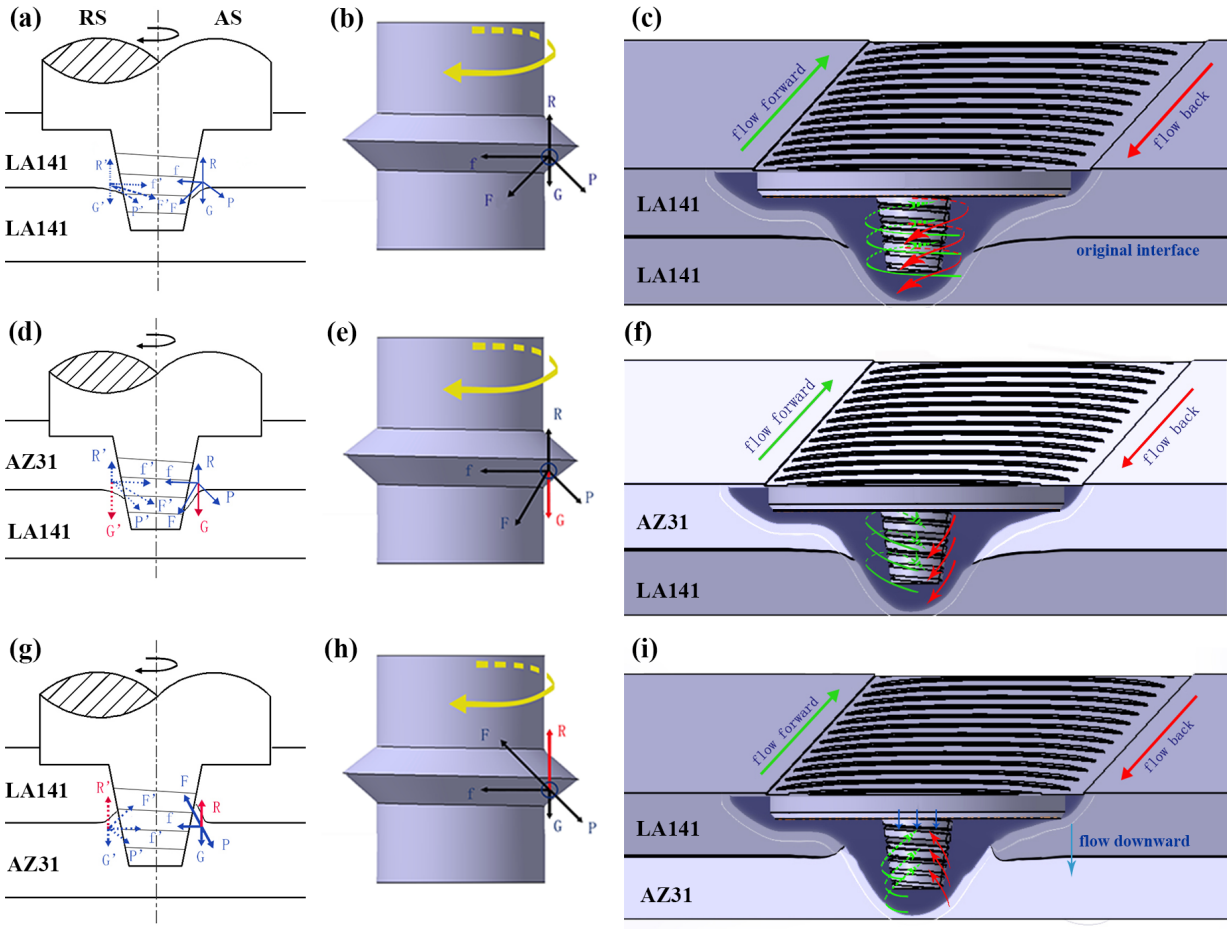

Figure 8: Diagram of (a) the F at the interface, (b) forces on the left thread surface and (c) material flow in the LA141/LA141 lap joint; diagram of (d) the F at the interface, (e) forces on the left thread surface and (f) material flow in the AZ31/LA141 lap joint; diagram of (g) the F at the interface, (h) forces on the left thread surface and (i) material flow in the LA141/AZ31 lap joint.

3.3 Interface migration characteristics of Mg-Li alloys FLSW

Different from many other similar FSLW joints of traditional Mg or Al alloys [17–19], the FSLW Mg-Li alloys joint appeared a hook defect that extended downward along the nugget boundary on the AS in this experiment. For the FSLW joint of Mg-Li alloys, the changing trend in the hook morphology would be account for the interface migration.

As the rotating tool pin traveling forward, the original lap interface in front of the pin had not been stirred. While the rotating pin came in contact with the material, it generated the enough heat and forced the material flow around the tool pin to refill the void created due to the tool movement [20]. The plasticized material flow was divided into horizontal flow and vertical flow, where the horizontal flow was the main flow, and the vertical flow was the secondary flow [21]. In other words, the material of the lower plate mainly refilled the empty of the lower plate, and the material of the upper plate mainly refilled the empty of the upper plate. The original lap interface in the stir zone experiencing a re-deformation may deviate from the original flat interface due to the material flow [22]. However, forces are the most essential causes of the material flow. Specifically, at the interface, they are critical for the interface migration and the weld quality [17, 24]. In this section, the interface migration characteristics were discussed based on the forces of the similar LA141 lap joint. Subsequently, they were further verified by different lap configurations (AZ31/LA141 and LA141/AZ31 joints).

The rotation of the pin is a fundamental source of forces [**?**]. Figure 8(b) is a schematic diagram of forces exerted on the plasticized metal at the LA141/LA141 lap interface, which were caused by the left thread of the pin during FSLW. The mechanical interaction, due to the velocity difference between the rotating tool and workpiece, produced rotary motion of plasticized material around it and created a frictional force (f) paralleled to the thread,

resulting in a downward pressure (p) perpendicular to the surface of the thread. In addition, forces at the interface were related to the physical properties of materials. The heat produced by the frictional work and material deformation, dissipated into surrounding materials, which led the temperature and materials to rise and plasticize, respectively. The plasticized metal was subject to the resistance (R) from un-softened metal and its own gravity (G). When the material was subjected to the enough heat, the forces in the plasticized pool reached a balance between G and support forces given by surrounding wall. Therefore, at the interface, G affecting the interface migration during FSLW was only related to the density of upper and lower plates. As the density of the upper plate was less than the lower plate, G had a slight effect during the similar lap welding. However, G significantly increased which was attributed to the higher density of the upper plate than that of the lower plate in the dissimilar lap welding. And according to the longitudinal temperature gradient, the value of R therefore gradually increased from top to bottom of the joint, since the gradient of force R was extremely related to the physical properties of the BM. In this study, the LA141 Mg-Li alloy has a lower melting point (580°C) and thermal conductivity (80 w/m·k) than that of other ordinary Mg alloys. During similar FSLW, the upper and lower plates had almost the same density, which lead to G at the interface had a slight effect on the interface migration. LA141 Mg-Li alloy with a low melting point in the stir zone was completely plasticized, and the relatively lower thermal conductivity presented a good temperature performance, which made the gradient of force R smaller. According to analysis shown in Figure 3(a), the original interface on the AS of the LA141/LA141 lap joint extended downwards along the boundary of the NZ, but on the RS, it extended slightly upwards into the NZ. It could be concluded that force R at the interface was little but slightly higher than G (Figure 8(b)). Under these four forces, forming a resultant force (F) on the AS towards the lower plate with about 45° as shown in Figure 8(a). Moreover, the f and p were correspondingly f' and p' on the RS. The f' was in opposition to f, but the p', R' and G' were in the same directions as the p, R and G. As a result, force F directed to the upper plate and the center of weld nugget, forming an angle of about 5° to the original faying interface (Figure 8(a) and 8(b)). As the tool traveling, the pin continuously transferred the plasticized material from the AS to the RS and then produced a hole on the AS. Subsequently, the hole was refilled by the plasticized material from the RS (Figure 8(c)). By the interaction with the rotating pin, the original interface was destroyed gradually and the plasticized material at the interface flowed well around the probe by the F with good temperature performance (Figure 8(c)). As a result, on the AS, the original interface of the LA141/LA141 lap joint extended downwards along the boundary of the NZ, however on the RS, it extended slightly upwards into the NZ as shown in Figure 3(a).

In order to verify whether the forces at the interface were critical factors in determining the interface migration during FSLW process, one of similar LA141 Mg-Li alloy plates was replaced with AZ31 Mg alloy plate. Comparing to the LA141 Mg-Li alloy, the AZ31 Mg alloy with a higher melting point (650°C) and thermal conductivity (155.5 w/m·k) has a poor plasticization. When the AZ31 plate was placed on top of the LA141 plate, it formed the AZ31/LA141 lap joint after FSLW (Figure 5(a)). At the lap interface, forces were changed because of the use of different materials. Compared with the LA141/LA141 lap joint, there was no obvious change in force R, but G significantly increased which was attributed to the higher density of AZ31 than that of LA141. As the material softened, G was much greater than force R and changed the direction of the F at the interface as shown in Figure 8(e). On the AS, the F pointed to the lower plate, approximately forming a bigger angle to the original faying surface. But on the RS, the F directed to the lower plate instead of the upper plate (Figure 8(d)). Under the effect of the F, the original interface moved downwards (Figure 8(f)). The hook morphology was like that of the LA141/LA141 lap joint but instead, the cold lap extended horizontally to the lower plate (Figures 5(a), 6(a) and 6(b)). The oxide layer behind the cold lap was transferred to the center of the lower plate by the F as shown in Figure 6(c) and 6(d).

Moreover, the AZ31 plate was placed on bottom of the LA141 plate, forming a LA141/AZ31 lap joint. Comparing with the LA141/LA141 lap joint, the heat of the lower plate possessing good dissipation was not enough to make the material completely plasticized for the FSLW LA141/AZ31 joint. As a result, the value of force R at the interface increased sharply but G at the interface was same as that of similar FSLW of LA141 Mg-Li alloy. Therefore, force R was higher than G. The F was therefore formed, pointing to the upper plate on the AS, and it also directed to the upper plate on the RS (Figure 8(g)). The original interface was moved upwards by F as shown in Figure 8(i), forming an upward hook and a cold lap which were demonstrated by Figure 6(b). In comparison with the AZ31/LA141 lap joint, the LA141/AZ31 lap joint was quite different and appeared a weld hole defect (Figure 6(b)). Because when the LA141 plate was used as the lower plate, the heat of the lower plate was enough to make it be fully plasticized. But the AZ31 plate which possessed a higher fusion point was introduced as the lower plate, resulting in a poor plasticized

material flow. The materials from the AS did not refill at the lower plate in time, while the cavity did not provide any upward supporting forces and then the fully plasticized LA141 Mg-Li alloy flowed to it under the action of G (Figure 8(i)), which agreed with the result of Figure 6(b).

Based on the results and analyses above, the f and p did not change under the same welding parameters, but different lap configurations altered force R and G. At the similar LA141 interface, the F on the AS pointed to the lower and that on the RS pointed to the upper plate during FSLW. Due to the change to the AZ31/LA141 lap joint, the F of both sides pointed to the lower plate, and the angle of the F on the AS became lager. However, in the LA141/AZ31 lap joint, the F on both sides pointed to the upper plate. As a result, different interface morphologies were formed because of various material flow behaviors under the F. At last, the FSLW joints appeared different interface migrations as a result of the forces above.

4 Conclusions

In this study, the feasibility of LA141 Mg-Li alloy FSLW and interface migration characteristics during FSLW process were investigated. The AZ31/LA141 and LA141/AZ31 lap joints were selected to verify the interface migration characteristics during FSLW. The following conclusions could be drawn:

(1) The LA141 Mg-Li alloy plates in similar lap configuration were successfully jointed using FSLW. The grain of the BM was about 30 μm, while after welding, in the NZ it was refined and was about 10 μm. Moreover, in the HAZ it grew up about 50 μm, and the grain in the TMAZ were elongated.
(2) The similar lap joint of LA141 Mg-Li alloy fractured at the interface defects, and the maximum lap-shear tensile testing load reached 2.8 kN.
(3) During FSLW, material flow was mainly affected by f, p, R and G, and interface migration was related to the F at the interface. The FSLW LA141/LA141 lap joints appeared a downward hook on the AS and an upward cold lap on the RS due to the interface migration as a result of the forces above. The FSLW of AZ31/LA141 and LA141/AZ31 furtherly verified that forces at the interface were critical factors in determining the interface migration during FSLW process.

Acknowledgement: This study was supported by the National Natural Science Foundation of China under Grant No. 51601121, and Liaoning Province Science Foundation Program No. L201624 and 201602570.

References

[1] H. Dong, F. Pan, B. Jiang and Y. Zeng, Mater. Des., 57(5) (2014) 121–127.
[2] T. Zhu, C. Cui, T. Zhang, R. Wu, S. Betsofen, and Z. Leng, Mater. Des., 57(1) (2014) 245–249.
[3] H. Wu, T. Wang, R. Wu, L. Hou, J. Zhang and X. Li, J. Mater. Process Technol., 254 (2018) 265–276.
[4] B. Ribic, T.A. Palmer and T. Debroy, Int. Mater. Rev., 54(4) (2013) 223–244.
[5] H. Li, D.L. Zhang, Y.X. Hou, X. Zhao and R.Z. Xu, Special Cast. Non. Alloy, 38(5) (2018) 543–547.
[6] J. Hiscocks, B.J. Diak, A.P. Gerlich and M.R. Daymond, Sci. Technol. Weld Join., 23(7) (2018) 1–7.
[7] M. Tsujikawa1, Y. Abe1, S.W. Chung, S. Oki, K. Higashi, I. Hiraki and M. Kamita, Mater. Trans., 47(4) (2006) 1077–1081.
[8] M. Bugdayci, A. Turan, M. Alkan, and O. Yucel, High Temp. Mater. Proc., 37(1) (2017) 1–8.
[9] H. Wu, T. Wang, R. Wu, L. Hou, J. Zhang, and X. Li, J. Mater. Process Technol., 254 (2018) 265–276.
[10] M. Besterci, K. Sülleiová, O. Velgosová, B. Balloková, and S.J. Huang, High Temp. Mater. Proc., 36(3) (2017) 279–283.
[11] R.Z. Xu, D.R. Ni, Q. Yang, C.Z. Liu and Z.Y. Ma, Sci. Technol. Weld Join., 22(6) (2017) 512–519.
[12] S. Ji, Y. Wang, Z. Li, L. Ma, L. Zhang and Y. Yue, High Temp. Mater. Proc. 36(7) (2017) 693–699.
[13] X. Cao, M. Jahazi, Mater. Des., 32(1) (2011) 1–11.
[14] S. Ji, Z. Li, J. Mater. Eng. Perform, 26 (2017) 1–10.
[15] S. Ji, X. Meng, J. Xing, L. Ma, and S. Gao, High Temp. Mater. Proc., 35(8) (2016) 843-851.
[16] W. Yuan, R.S. Mishra, B. Carlson, R. Verma, and R.K. Mishra, Mater. Sci. Eng. A, 543(5) (2012) 200–209.
[17] S. Ji, Z. Li, Y. Wang, L. Ma, and L. Zhang, High Temp. Mater. Proc., 36(5) (2016) 495–504.
[18] Y. Hu, H. Liu, and S. Du, Metall. Mater. Trans. A, 49(8) (2018) 3321–3332.
[19] Q. Wen, Y. Yue, S. Ji, Z. Li, and S. Gao, High Temp. Mater. Proc., 35(4) (2016) 375–379.
[20] W. Li, Z. Liang, and C. Cai, High Temp. Mater. Proc., 37(7) (2018) 675–681.
[21] Z. Lai, C. Pan, H. Du, X. Chen, R. Xie, and L. Liu, Sci. Technol. Weld Join., 23(1) (2017) 1–9.
[22] M. Reimann, J. Goebel, J.F.D. Santos, Mater. Des. 132 (2018) 1–7.
[23] X.H. Zeng, P. Xue, D. Wang, D.R. Ni, B.L. Xiao, K.S. Wang and Z.Y. Ma, Sci. Technol. Weld Join., 23(8) (2018) 677–686.
[24] X. Song, L.M. Ke, J.X. Liao, L. Xing, and C.P. Huang, Journal of Nanchang Hangkong University, 26(4) (2012) 78–82.